GeoPlanning
Journal of Geomatics and Planning
Geoplanning: Journal of Geomatics and Planning, Vol. 12, No. 2, 2025, 215 - 238

e-ISSN: 2355-6544

Received: 07 February 2025;
Revised: 17 July 2025;
Accepted: 25 October 2025;
Available Online: 31 October 2025;
Published: 31 October 2025.

Keywords:
Freshwater Lakes; Geospatial Techniques; Principal Component Analysis; Spatio-Temporal Analysis; Weighted Overlay

*Corresponding author(s)
email: aekbal@uitm.edu.my

Original Research Open access

Empirical Evidence of Environmental Degradation Using Geospatial Technology in Tasik Temenggor, Royal Belum Perak, Malaysia

Kamilia Kamaruzzaman[1], Siti Aekbal Salleh*[2,3], Faezah Pardi[3], Muhammad Fuad Abdullah[3], Vladimir Foronda[4], Zulfadhlan Ahmad Khushairi[5], Muhamad Soleh Abu Hassan[5], Nazri Che Dom[2,6]

1. *3DTech Parametric Sdn Bhd, Menara Uncang Emas, 3, Taman Miharja, 55200 Kuala Lumpur, Malaysia.*
2. *School of Geomatics Science and Natural Resources, College of Built Environment, Universiti Teknologi MARA (UiTM), 40450 Shah Alam, Selangor, Malaysia,*
3. *Institute for Biodiversity and Sustainable Development (IBSD), Universiti Teknologi MARA, 40450, Shah Alam, Selangor, Malaysia,*
4. *College of Agriculture and Natural Resources, Central Bicol State University of Agriculture, Camarines Sur, Pili, Philippines*
5. *Pulau Banding Foundation, 47850 Petaling Jaya, Selangor, Malaysia.*
6. *Faculty of Health Sciences, Universiti Teknologi MARA (UiTM), UITM Cawangan Selangor, 42300 Puncak Alam, Selangor, Malaysia.*

DOI: 10.14710/geoplanning.12.2.215-238

Abstract

Freshwater ecosystems are vital ecosystems for life, but in reality, they face severe pressure from anthropogenic activities, climate change, and land use changes. These conditions cause the environmental degradation process to accelerate, as is the case in Lake Temenggor, Malaysia. This study examines environmental degradation in Tasik Temenggor, Malaysia, using geospatial techniques to analyze land surface temperature (LST), normalized difference vegetation index (NDVI), land use and land cover (LULC), water quality, and air temperature. The aim of this study is to identify factors associated with environmental degradation, specifically focusing on climate and meteorological parameters and analyzing their temporal changes through spatio-temporal analysis. Data used were obtained from Landsat 8 OLI/TIRS and field observations, processed using ArcGIS Pro with Principal Component Analysis (PCA) and Weighted Overlay Analysis (WOA). The results show increasing degradation in agricultural and development areas, while forest zones remain relatively stable. Consistent LST classification is applied across all years to ensure valid temporal comparisons. The integration of PCA and WOA demonstrates a robust methodological framework that supports effective environmental monitoring. These findings highlight the practical utility of geospatial techniques in conservation planning and suggest targeted interventions for high-risk areas. In conclusion, this study demonstrates the application of geospatial technology in monitoring and assessing environmental degradation in Tasik Temenggor.

1. Introduction

Freshwater resources are critical to both natural ecosystems and human development. They are necessary for industry, agriculture, and human survival in general (Tibebe et al., 2022). In addition, freshwater ecosystems provide vital services to both the environment and people (Albert et al., 2021). At local, regional, and global

levels, the characteristics and volume of freshwater play a crucial role in shaping biogeochemical processes and ecological interactions. These factors ultimately impact biodiversity, the productivity of ecosystems, as well as human health and well-being (Albert et al., 2021; Kamaruzzaman et al., 2025). Moreover, freshwater ecosystems constitute a vital element within diverse habitats, recognized as pivotal strategic assets for supporting human sustenance, fostering economic progress, and preserving the environment (Kamaruzzaman et al., 2025; Razak et al., 2020). However, biodiversity in freshwater habitats is diminishing swiftly across all continents and major river basins globally, and this decline is occurring at a faster rate compared to terrestrial ecosystems (Albert et al., 2021; Pratama et al., 2022).

Situated in the eastern part of Perak, Malaysia, Temenggor Lake is considered by tropical rainforests and holds the distinction of being the second-largest lake on the Peninsular Malaysia (Razak et al., 2020). Positioned approximately 45 kilometers away from the district capital, Gerik, Temenggor Lake is a human-made reservoir formed during the 1960s and 1970s. Renowned for its breathtakingly natural beauty and diverse ecological tapestry, this reservoir serves as a crucial habitat for a myriad of flora and fauna, including numerous endemic and rare species. However, this once pristine ecosystem now faces a multitude of environmental challenges that threaten its sustainability and the well-being of the species it sustains. The significant ecological threat to Tasik Temenggor arises from the rapid increase in invasive aquatic plant species, namely water hyacinth and giant salvinia. This aligns with the assertion that water hyacinth, scientifically known as Eichhornia crassipes, originated in the Amazon basin and has quickly proliferated globally (Godana et al., 2022). It is an invasive aquatic plant with various ecological and economic implications in freshwater ecosystems.

The challenges are further compounded by various threats posed by human activities, including land reclamation, habitat deterioration, and eutrophication (Martinsen & Sand-Jensen, 2022). Furthermore, the escalation of population growth, changes in agricultural practices, and increased sewage runoff from urban areas have significantly elevated nutrient inputs beyond their natural levels in recent decades, consequently accelerating the process of eutrophication (Tibebe et al., 2022). Moreover, the ecological well-being and endurance of lakes have faced significant threats since the early 20th century, primarily due to swift urbanization, global climate change, and heightened human activities (Ho & Goethals, 2019). Furthermore, human activities are changing the patterns and movements of surface, subsurface, and atmospheric waters on a regional scale, compromising the resilience of aquatic, riparian, and coastal ecosystems (Rodell et al., 2018). These effects have placed Tasik Temenggor ecosystem under immense pressure, raising concerns about its long-term viability and the preservation of its unique biodiversity. Additionally, Temenggor Forest Reserve is concerned about heavy metal pollution in Tasik Temenggor (Arshad et al., 2022). Elevated Heavy Metal Pollution Index (HPI) and Metal Index (MI) readings indicate potential contamination hazards in water samples, showing that heavy metal pollution has affected specific locations in Tasik Temenggor.

Similar cases have been reported in other countries, highlighting a global pattern of freshwater degradation. For example, large-scale aquatic vegetation decline has been observed in Ethiopia's Lake Dambal (Godana et al., 2022), habitat fragmentation has intensified in China's lake basins (Zhou et al., 2022), and cropland abandonment around freshwater lakes in Vietnam has exacerbated erosion and nutrient runoff (Karim et al., 2023). Additionally, India, Brazil, and other biodiversity-rich nations have documented significant impacts from unplanned land-use changes and water pollution (Ho & Goethals, 2019; Liu et al., 2020). These international parallels underscore the urgency for robust, scalable monitoring techniques that can detect environmental change with precision.

While past research has addressed environmental threats in Tasik Temenggor, most studies focus on isolated parameters such as land cover change or water chemistry. There is a lack of integrated, spatio-temporal assessments that combine vegetation indices, surface temperatures, land use, and water quality to understand the cumulative nature of degradation. Moreover, few studies have systematically quantified these variables across multiple time periods using advanced geospatial techniques (Kowe et al., 2023; Kumar et al., 2022; Topp et al., 2020). This research addresses that gap by employing satellite-derived datasets and in-situ measurements to evaluate environmental degradation over the years 2015, 2020, and 2024.

Hence, understanding the extent and severity of these threats is paramount to develop effective conservation and management strategies to safeguard this valuable natural resource. To effectively address the environmental challenges faced by Tasik Temenggor, a comprehensive understanding of its ecological profile is essential. Therefore, it is crucial to set up a new baseline that shows how the conditions in the Temenggor Lake area have changed over time due to environmental degradation. Producing spatio-temporal maps that depict these changes over time will help decision-makers make informed decisions about conservation strategies, considering the degree of environmental degradation (Nisar et al., 2023). However, managing and reversing the challenges presented including biodiversity decline, degradation of water quality, impact on economic development, and implications for human well-being, proves to be a complex task (Razak et al., 2020).

Therefore, this study will be conducted by using geospatial technologies. Geospatial technology, which includes Geographical Information Systems (GIS) and Earth Observation (EO), is an important tool and method for quantifying changes over time and space (Kowe et al., 2023; Salleh et al., 2014; Salleh et al., 2015). The use of remote sensing technology for its potential to overcome time constraints, accessibility challenges, and cost issues associated with traditional water sampling techniques, becomes particularly valuable (Kowe et al., 2023). Additionally, remote sensing can complement in-situ measurements, addressing the challenges in monitoring water quality (Muchini et al., 2018). Moreover, there is broad utilization of remotely sensed imagery for accurate quantification of variations in water quality (Topp et al., 2020). Geospatial technology offers a powerful tool to enhance the monitoring and management of environmental degradation in Tasik Temenggor. Satellite imagery and Geographic Information Systems (GIS) can provide valuable spatial data such as land use changes within the catchment area. A comprehensive understanding of the spatial and temporal dynamics of environmental degradation in the lake and its surroundings can be obtained.

The novelty of this study lies in its methodological integration of Principal Component Analysis (PCA) and Weighted Overlay Analysis (WOA) within a GIS framework to produce spatial degradation maps with high temporal resolution. By synthesizing variables such as NDVI, LST, LULC, water quality, and air temperature, the study provides a comprehensive model to monitor ecological shifts in freshwater ecosystems. The aim of this study is to identify factors associated with environmental degradation, specifically focusing on climate and meteorological parameters and analyzing their temporal changes through spatio-temporal analysis. The primary objectives of the study are to (i) identify significant environmental degradation variables, (ii) quantify their influence using spatial and statistical tools, and (iii) generate spatio-temporal degradation maps that can inform conservation strategies. This approach not only enhances local environmental assessment but also contributes a transferable model for monitoring freshwater ecosystems elsewhere

2. Data and Methods

The methodology of this project is divided into four (4) main phases which is i) desk literature ii) data collection, iii) data processing, and iv) result and analysis. Figure 1 shows the flow of work for the study that has been implemented. Research questions and objectives have been defined during the first phase of the study, setting an outline for the entire study. Next, the systematic literature review also has been completed to identify the parameters needed for this research. This critical phase includes identifying the study area, which is Tasik Temenggor in Perak. Furthermore, the software to be used has been selected.

The next phase involves the process of data collection. Acquiring satellite imagery took center stage where 3 satellite images were downloaded which include 2015, 2020 and 2024. Notably, the satellites chosen were Landsat 8 OLI/TIRS. The Landsat image was downloaded from the open-source U.S Geological Survey (USGS) website. The next step for this research is reproduction of spatial data where LULC, LST, NDVI, air temperature and water quality data were produced. Spatial data reproduction starts with the image pre-processing. The image pre-processing includes radiometric correction for Landsat satellite imagery. Then, supervised classification was carried out. These classifications are pivotal for subsequent analyses, including LULC, LST, NDVI, air temperature and water quality, utilizing the acquired images. It is important that images from each year within the specified timeframe from 2015, 2020, and 2024 will undergo identical processing steps.

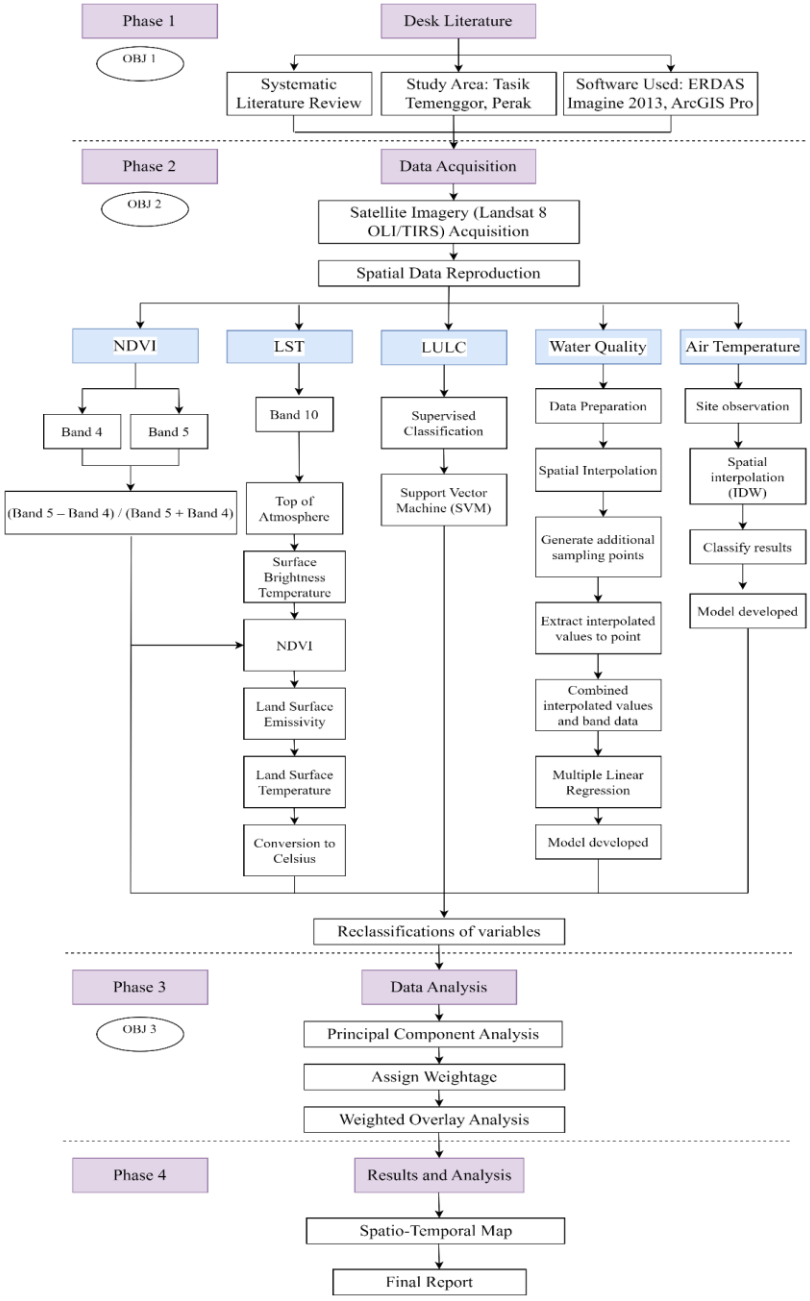

Figure 1. Workflow of the Study

After obtaining the results, all of these will be the parameters to conduct the environmental degradation analysis. Prior to proceeding with the further processing, ensure that all the parameters are classified into relevant and readable data. Therefore, the Principal Components tools in ArcGIS Pro assigned weights to variables' parameters, and after acquiring all weights, the Weighted Overlay Analysis tool is used to allocate percentage weighting to each layer. This results in three distinct maps illustrating the environmental condition in Tasik Temenggor over the years 2015, 2020, and 2024. The final output then be reclassified into five categories to better understand the varying degrees of environmental condition within the study area. The last phase involves results and analysis where the final product of this research was map showing the level of environmental condition at the study area. Upon analyzing the spatio-temporal map, we will conclusively determine the area's degradation status. Hence, this study is conducted to measure and assess the elements contributing to environmental degradation.

2.1. Desk Literature

Through this phase, research questions and objectives have been set up, providing a framework for the entire study. Hence, the first objective of the study is to quantify the factors of environmental degradation followed by the second objective which is to conduct a spatio-temporal analysis of the changes of the environmental factors. Additionally, a study area and software used has been determined. Subsequently, a systematic review of the existing literature was conducted to identify the parameters essential for inclusion in this research. This systematic literature review has been conducted by using VOSviewer tools to construct and visualize bibliometric networks. These networks include the keywords from the publications. Finally, to ensure the success of this study, the determined software must involve every phase from data collection until result and analysis.

2.2. Study Area

Tasik Temenggor (see Figure 2) is a man-made lake located in the Hulu Perak district of Perak, Malaysia. It was created in 1974 with the construction of the Temenggor Dam, which is a hydroelectric dam that generates electricity for the states of Perak and Penang. The lake is home to a variety of flora and fauna, including the Temenggor tiger, which is a critically endangered subspecies of tiger. Tasik Temenggor is part of the Royal Belum State Park, which is the largest virgin rainforest in Peninsular Malaysia. The park is home to a wide variety of plant and animal species, including more than 1,000 species of trees, 600 species of birds, and 100 species of mammals. However, Tasik Temenggor is facing increasing threats from deforestation, logging, agricultural expansion, pollution, and tourism (Albert et al., 2021; Arshad et al., 2022; Razak et al., 2020). These pressures are having a significant impact on the ecosystem, leading to declining forest cover, decreasing wildlife populations, and deteriorating water quality (Ho & Goethals, 2019; Pratama et al., 2022; Rodell et al., 2018).

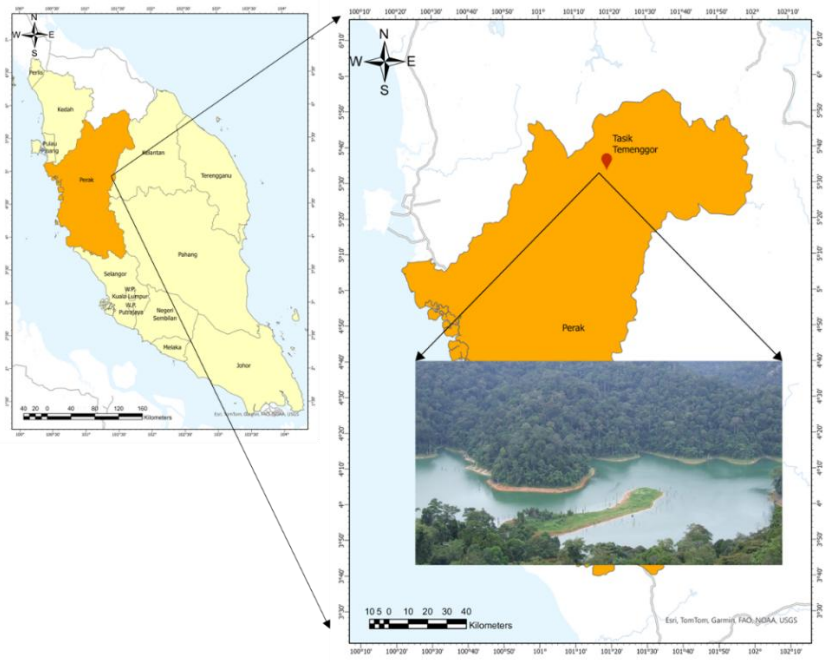

Figure 2. Study Area

2.3. Data Acquisition

Data acquisition is the process of gathering and organizing information. The data information is chosen based on the research needs. Data collection is an important task that serves as the project's pillar. The data collected for this study is of various types and sources. Table 1 shows the data acquisition for this study.

Table 1. Data Acquisition

No	Data Type	Description	Source
1	Satellite Imagery – Landsat 8 OLI/TIRS	Year 2015, 2020, and 2024	USGS Explorer
2	Study Area – Tasik Temenggor	Shapefile	DIVA-GIS
3	In-situ measurement (Water Quality)	Turbidity, pH, Temperature, DO, BOD, TSS, NH-3	Secondary Data

In this study, data acquisition consisted of several key components, including satellite imagery, spatial data processing, and in-situ measurement. Acquiring satellite imagery took centre stage where three (3) satellite images has been downloaded which include year 2015, 2020 and 2024. Notably, the satellites chosen were Landsat 8 OLI/TIRS. These imageries were acquired from open source United States Geological Survey (USGS). These images were used to aid in the identification of land use and land cover (LULC) changes, analysis of normalized difference vegetation index (NDVI), analysis of land surface temperature (LST), and evaluation of water quality and air temperature in the study area. The objective is to generate spatio-temporal maps that depict the changing levels of environmental deterioration during the designated years. Table 2 shows the Landsat 8 properties for the image used in 2015, 2020 and 2024.

Table 2. Satellite Image Properties

Year	Landsat ID	Cloud (%)
2015	LC08_L1TP_127056_20150919_20200908_02_T1	6.08
2020	LC08_L1TP_127056_20200308_20200822_02_T1	3.34
2024	LC09_L1TP_127056_20240514_20240514_02_T1	19.77

Subsequently spatial data processing, where in this study it was conducted through a series of integrated analytical procedures designed to improve data quality and extract relevant environmental indicators from satellite imagery. The procedures encompassed satellite image pre-processing, vegetation analysis, land surface temperature analysis, land use classification, and the integration of remotely sensed data with in-situ measurements to assess environmental conditions in the study area.

Prior to initiating data processing, a crucial first phase involved data pre-processing. This procedure was essential for maintaining data integrity and improving its practicality. Hence, the pre-processing stage encompasses the preparation of data from satellite image which is Landsat 8 OLI/TIRS. Initially, the satellite images have been stacked. Following this, corrections which is radiometric corrections, are implemented. This method was crucial to guarantee that the data was in its reliable condition, clear of any disturbances caused by other atmospheric distortions. The main objective was to ensure the utmost quality of the output derived from Landsat data, facilitating precise and significant data analysis.

After pre-processing the satellite image, it is feasible to compute the Normalized Difference Vegetation Index (NDVI) using raster calculator tools in ArcGIS Pro. Equation 1 shows the algorithm utilized for NDVI calculation. This index is determined by taking the difference between Band 5 and Band 4 and dividing it by the sum of Band 5 and Band 4 For Landsat 8 OLI/TIRS. Band 5 corresponds to the near-infrared band, and band 4 corresponds to the red band. Study from Nagy et al. (2021) was referred to conduct the NDVI calculation as below in Equation 1:

$$NDVI = \frac{(Band\ 5 - Band\ 4)}{(Band\ 5 + Band\ 4)} \quad \text{.....(Equation 1)}$$

Elevated values in the Normalized Difference Vegetation Index (NDVI) within the 0 to 1 range signify the existence of diverse, thriving, and green vegetation cover. The process of extracting and classifying the NDVI was categorized into 5 distinct classes which is Dense Vegetation, Moderate Vegetation, Sparse Vegetation, Bare soil, and Water.

Thereafter, land surface temperature (LST) was estimated to examine the thermal characteristics of the Earth's surface, calculated based on measured radiance, is referred to as Land Surface Temperature (LST). It is derived from solar radiation, and the surface is defined from a satellite perspective by what is visible when looking through the atmosphere to the ground. LST plays an important role in determining the thermal properties of the Earth's surface, influencing its effective radiating temperature. Landsat 8 OLI/TIRS images can provide critical information about Land Surface Temperature. This data is critical for mapping and monitoring temperature-related events on the Earth's surface. The images obtained will then be process using ArcGIS Pro software to calculate the LST. Study from Kumar et al. (2022) has been referred to conduct the LST calculation. The calculation of LST involve six (6) crucial step which begin with the calculation of Top of Atmosphere (TOA), Surface Brightness Temperature (SBT), calculation of NDVI, Land Surface Emissivity (E), and finally, the calculation of LST. Raster Calculator tools has been utilized to calculate all LST. After the calculation of LST has been obtained, the conversion from Kelvin to Celsius has also be accomplished.

Furthermore, to vegetation and thermal analysis, land use and land cover (LULC) classification was performed using supervised classification techniques in ArcGIS Pro. Initially, satellite imagery is launched into the software after it has been pre-processed. At the root of supervised classification is the collection of training samples, in which specific areas representing various land cover classes are identified. These samples are used to train the classification algorithm, with spectral signatures extracted to represent the reflectance or radiance of the pixel in different bands. The Classification toolset in the ArcGIS Pro Toolbox is used to select the preferred algorithm, such as Maximum Likelihood or Support Vector Machine. Thus, Support Vector Machine has been used in this study due to its credibility for providing more effective classification accuracies in land cover classification applications (Xie & Niculescu, 2021). Additionally, previous successful applications of SVM in land cover classification problems, as evidenced in papers such as Tran et al. (2015) contribute to its selection for this study. Using the collected samples, the algorithm is then trained to learn the spectral characteristics of each land cover class. When the trained classifier is applied to the entire image, it produces a classified image in which pixels are assigned specific land cover classes. This analysis is conducted using imagery acquired in the years 2015, 2020, and 2024 earlier.

In addition, water quality analysis is conducted by integrating Landsat 8 satellite imagery, which enables monitoring of water quality parameters by combining remote monitoring with field observations. The study utilised Landsat 8/9 OLI/TIRS images to gather reflectance values for each band, which were then correlated with field-measured data. Regression analysis was employed to find the best model to predict important water quality metrics. The integration of satellite data with on-site measurements facilitated the development of precise models for estimating water quality parameters. This study demonstrated the ability of remote sensing in offering significant insights for monitoring water quality. Table 3 depicts the locations of field-measured data that has been obtained as the secondary data. There are total of six (6) locations (see Table 3).

Table 3. Location of Sampling Points

No	Station/Location	Latitude	Longitude
1	Kg. Sungai Ta'hain	5.747500	101.390833
2	Kg. Klewang	5.680359	101.409440
3	Kg. Sungai Tiang	5.695500	101.442400
4	Houseboat Park Sg. Ko'oi	5.666759	101.399956
5	Houseboat Park Sg. Papan Luar	5.638055	101.370555
6	Houseboat Park Sg. Ruok	5.595114	101.377868

The study involved analyzing water quality by integrating in-situ data with Landsat 8/9 imagery. First, in-situ water quality readings from 2020, along with their geographic coordinates, were compiled into a CSV and imported into ArcGIS Pro as a point feature class. Landsat imagery for the same period was pre-processed using ERDAS Imagine and ArcGIS Pro to correct for atmospheric conditions and remove cloud cover. Due to the limited number of sampling points, the Inverse Distance Weighting (IDW) method was used to interpolate

the data, creating a raster surface for various water quality parameters. To generate more sampling points, a fishnet grid was created using the Create Fishnet tool, and interpolated raster values were extracted to these points. Both in-situ and Landsat data were aligned to the same coordinate system, and the Extract Multi Values to Points tool was used to combine the data. Finally, multiple linear regression was performed using SPSS Statistics to predict water quality based on Landsat bands, with results including Model Summary, ANOVA, and Coefficient tables to assess the model's fit and the contribution of each band.

Furthermore, air temperature analysis was incorporated to complement the assessment of environmental degradation. Air temperature is closely associated with vegetation conditions, land use changes, surface temperature, and water quality. Air temperature can be closely related to NDVI, land use, LST, and water quality to monitor environmental degradation efficiently. Higher air temperatures can stress vegetation, lowering NDVI values, and changes in land use, like urbanization, can increase local temperatures, creating urban heat islands. LST, reflecting surface heat absorption, can indicate surface changes such as deforestation and urbanization. Higher air temperatures also affect water quality by altering water temperatures, decreasing dissolved oxygen, and promoting harmful algal blooms. Integrating air temperature data with NDVI, land use, LST, and water quality data provides a comprehensive view of environmental changes, revealing patterns and trends over time and across regions. Air temperature data were recorded using TinyTag data loggers at Tasik Temenggor on 14 May 2024 and compiled into a CSV file containing geographic coordinates and temperature values. The data were imported into ArcGIS Pro as point features, and a continuous surface was generated using Inverse Distance Weighting (IDW) interpolation. The resulting raster was classified into five categories—very low, low, moderate, high, and very high. Subsequently, air temperature prediction followed a procedure similar to that used for water quality modeling, in which Landsat 8/9 OLI/TIRS reflectance values were correlated with field-measured data using regression analysis to develop predictive models for the years 2015 and 2020.

Once the parameter for the environmental degradation monitoring had been derived, the resulting NDVI and LST layers were further reclassified to enhance interpretability and facilitate comparative analysis. Reclassification was performed using the Manual Interval classification methods in ArcGIS Pro. Both parameter for NDVI and LST is divided into five (5) distinct groups. The process of reclassification is performed using the "Reclassify" Tool in ArcGIS Pro, which consists of five classifications. For example, classification involving Very Low, Low, Moderate, High, and Very High has been applied for LST. Meanwhile, NDVI was categorized into 5 distinct classes which is Dense Vegetation, Moderate Vegetation, Sparse Vegetation, Bare soil, and Water. This multi-class categorization not only contributes to visual clarity but also establishes a nuanced framework for understanding the varying degrees of environmental condition within the study area.

2.4. Data Analysis

Data Analysis is the third phase in conducting this study. This study undergoes a few processing steps before obtaining the results where all the parameters obtained in Phase 2 has been assign the weightage by using Principal Component Analysis (PCA) and then Weighted Overlay Analysis was utilized to obtain the final output of spatio-temporal map (Kowe et al., 2023; Kumar et al., 2022; Topp et al., 2020).

Principal Component Analysis (PCA) was utilized to simplify complex datasets and highlight the most significant patterns or trends. PCA is a statistical method for dimensionality reduction and data compression. It transforms the original variables into a new set of uncorrelated variables known as principal components, which capture the data's maximum variance. PCA is commonly used in various fields, such as data analysis, image processing, and machine learning. The Principal Components tools in ArcGIS Pro were used to assign weights to the parameters of each variable. Therefore, this analytical procedure determines the weights assigned to each parameter inside the variables.

After acquiring all parameter weights through Principal Component Analysis, the Weighted Overlay Analysis tool is utilised. The allocation of percentage weighting to each layer is incorporated throughout this stage. The outcome comprises three distinct maps corresponding to the years 2015, 2020, and 2024. Therefore, a spatio-temporal map illustrating the extent of degradation in Tasik Temenggor has been generated.

3. Results and Discussion

The results of Normalized Difference Vegetation Index (NDVI), Land Surface Temperature (LST), Land Use Land Cover (LULC), Water Quality and Air Temperature were presented in this section. The final output for this study was also presented where map showing the level environmental condition in Tasik Temenggor after all the parameters has been calculated. After analyzing the map, we will be able to identify the area's deterioration condition. Additionally, Principal Component Analysis (PCA) has been utilized to assign weightage to each of the parameters before obtaining the final step using Weighted Overlay Analysis.

3.1. Normalized Difference Vegetation Index (NDVI)

The output shows a complex and varied environment composition of NDVI in year 2015, 2020 and 2024 (see Table 4). In 2015, with 2.63% of the land covered by bodies of water, the region is highly significant for aquatic ecosystems. However, some of the water bodies area was found to become bare soil. This might be because actual water was in a murky condition. Hence, the NDVI results has classified it as a bare soil. The percentage of bare soil (0.73%) denotes regions with little to no vegetation, maybe as a result of natural or man-made processes including land degradation or deforestation. Additionally, 4.74 percent of the land is covered by sparse vegetation, which indicates places with less dense or difficult-to-establish vegetation which could possibly be result of low-quality soil or insufficient water availability. With moderate vegetation making up 81.80% of the land, the area appears to have a generally stable and healthy vegetation cover that sustains the regional biodiversity and maintains the ecological balance of the area. Dense vegetation makes up 10.09% of the total, indicating areas with ideal growth circumstances and little disturbance.

Table 4. Results of NDVI

Year	NDVI Class	Area (ha)	Percentage (%)
2015	Water	13,355.70	2.63
	Bare Soil	3,728.23	0.73
	Sparse Vegetation	24,096.50	4.74
	Moderate Vegetation	415,757.00	81.80
	Dense Vegetation	51,304.80	10.09
2020	Water	10,452.10	2.06
	Bare Soil	5,610.59	1.10
	Sparse Vegetation	43,567.60	8.57
	Moderate Vegetation	391,403.00	77.01
	Dense Vegetation	57,184.60	11.25
2024	Water	15,414.28	3.03
	Bare Soil	1,162.02	0.23
	Sparse Vegetation	24,488.90	4.82
	Moderate Vegetation	342,966.50	67.48
	Dense Vegetation	124,219.90	24.44

Additionally, in 2020, water bodies occupy 2.06% of the area, the region's aquatic ecosystems are highly significant. Nonetheless, there has been a rise in the number of areas classified as bare soil, most likely as a result of water bodies being misclassified by the NDVI because of their murky state. 1.10% of the land is presently covered in bare soil, which denotes regions with little to no vegetation, perhaps as a result of human or natural processes like degradation of land or deforestation. Compared to 2015, the percentage of sparse vegetation has increased to 8.57%, indicating areas with less dense or struggling plants because of things like low soil quality or insufficient water. Slightly less than in 2015, moderate vegetation makes up 77.01% of the land, suggesting a generally maintained and healthy vegetation cover. 11.25 percent of the land is covered by dense vegetation, which denotes regions with ideal growth conditions and little disturbance.

Water bodies now cover 3.03% of the region, indicating a higher presence than in previous years, underscoring the significance of the aquatic ecosystems. Conversely, the areas classified as bare soil have significantly decreased to 0.23%, much lower than in 2015 and 2020. The percentage of sparse vegetation, which had declined in 2020, has increased to 4.82% in 2024, compared to 8.6% in 2020. Moderate vegetation covers 67.48% of the land, less than in 2015, indicating a generally maintained and healthy vegetation cover. Meanwhile, dense vegetation now occupies 24.4% of the area, a substantial increase compared to 2020, reflecting improved growth conditions and reduced disturbance.

Figure 3 below offers a detailed depiction of the environmental composition of the study area and displays the visualization of these data in 2015, 2020 and 2024. The geographical distribution of the region's water bodies, bare soil, sparse, moderate, and dense vegetation is depicted on this map. A better understanding of the distribution and temporal evolution of these different land cover categories can be obtained by looking at the map.

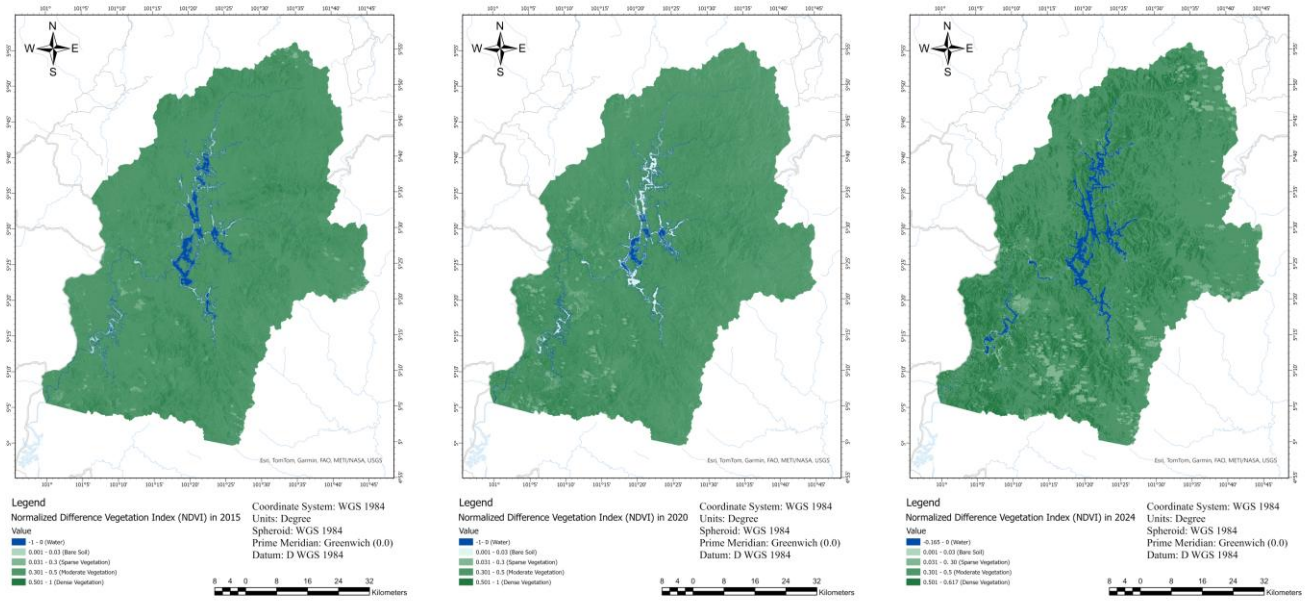

Figure 3. Results of NDVI for 2015, 2020 and 2024

3.2. Land Surface Temperatures (LST)

Notably, 86.85% of the studied area had moderately low temperature levels (see Table 5). The NDVI data for 2015 suggested that this region had moderate vegetation. Furthermore, 12.53% of the research area had low LST values, and this part of the region had mostly classified as forest for the LULC results in 2015. Further analysis reveals that 0.42% of the area experienced moderately high LST values. In 2015, this area corresponded to moderate NDVI ranges with some regions showing classification of developed area (residential area) for LULC. Moreover, 0.19% of the study area was identified as having very low LST values. This region was associated with forest in 2015, however, this result might be due to the presence of clouds too. Lastly, a very small portion of the study area, accounting for only 0.01%, exhibited high LST values. This region was characterized as bare soil according to the NDVI and LULC data from 2015. These findings underscore the intricate relationship between LST and vegetation cover, highlighting how varying degrees of vegetation influence temperature distribution across the study area.

Additionally, in 2020, 56.51% of the research area had very low LST values, and the NDVI suggested moderate vegetation while LULC results in 2020 shows it was an area with forest and little bit of cultivated area. In addition, 42.90% of the land had low LST values, which corresponded to places with moderate to thick vegetation. Furthermore, 0.54% of the study area experienced moderately low LST values, where the NDVI

indicated a mix of moderate and some dense vegetation. Finally, a small portion of the area with 0.17%, exhibited moderately high LST values and this area comprised a mix of sparse and moderate vegetation as well as classified as bare soil for LULC in 2020.

Specifically, in 2024, 68.49% of the study area exhibited moderately low LST values, with the LULC results indicate the regions as forest. Additionally, 24.02% of the study area had moderately high LST values, which were associated with planted or cultivated area. Furthermore, 6.29% of the area experienced low LST values, where the LULC results in 2024 shows it forest area. A small portion, 1.06%, exhibited high LST values, which corresponded to areas with bare soil. Lastly, 0.04% and 0.1% of the study area had very low LST values and very high LST value, respectively.

Table 5. Results of LST

Year	LST Class	Area (ha)	Percentage (%)
2015	Very Low	944.816	0.19
	Low	63,704.00	12.53
	Moderately Low	441,442.00	86.85
	Moderately High	2,153.21	0.42
	High	18.05	0.01
2020	Very Low	287,182.00	56.51
	Low	218,283.00	42.90
	Moderately Low	2,761.05	0.54
	Moderately High	8.85	0.15
2024	Very Low	189.03	0.04
	Low	31,979.92	6.29
	Moderately Low	348,134.60	68.49
	Moderately High	122,091.10	24.02
	High	5,364.04	1.06
	Very High	504.59	0.10

Figure 4 below offers an interpretation of the Land Surface Temperature (LST) distribution in the study area and visualizes these data effectively.

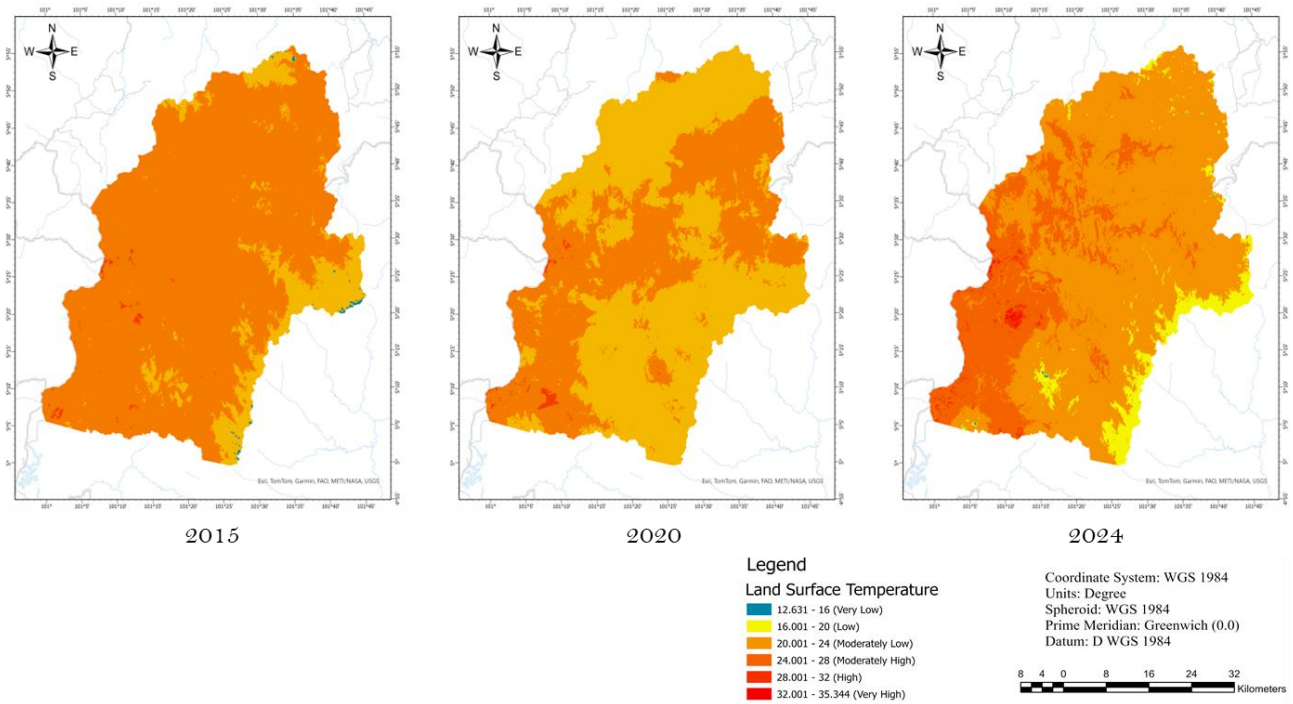

Figure 4. Results of LST for 2015, 2020 and 2024

3.3. Land Use Land Cover (LULC)

Table 6 shows the overall results for LULC data processing. The data reveals that forested areas overwhelmingly dominate the landscape, covering 79.92% of the region. This substantial forest cover indicates the presence of extensive natural vegetation. Planted or cultivated lands represent the second largest category, occupying 7.87% of the area, reflecting agricultural activities within the region. Barren land accounts for 7.16% of the area, indicating regions with minimal vegetation, possibly due to natural or anthropogenic factors such as soil degradation or land clearing. Water bodies, essential for local ecosystems, make up 4.41% of the area, showcasing the aquatic features within the landscape. Finally, developed areas constitute a mere 0.65% of the total land, signifying limited urbanization or infrastructural development in 2015. This detailed analysis of LULC provides crucial insights into the spatial distribution and extent of different land cover types, offering a baseline for understanding environmental changes.

Furthermore, according to the table, in 2020 forested areas dominate the landscape, covering 78.62% of the region, although this represents a decline from previous years. The second largest land cover is planted or cultivated areas, accounting for 11.71% of the total area. Barren land occupies 4.64% of the study area, which also marks a decrease compared to earlier analyses. Water bodies and developed areas make up 3.89% and 1.14% of the land, respectively. There has been a decline in the percentage of water bodies, likely indicating changes in water availability or quality, while the developed areas have shown an increase, reflecting ongoing urbanization or infrastructure development. These shifts in land cover categories highlight the dynamic changes occurring in the region, emphasizing the need for continuous monitoring to effectively manage and conserve the environment. The detailed analysis provides valuable insights into the temporal and spatial patterns of land use and cover, aiding in the understanding of the region's ecological health and trends. As indicated in the table, in 2024, the forested areas dominate the landscape, covering 78.73% of the region, which shows minimal change from previous years, specifically 2020. The second most prevalent land cover is the planted or cultivated areas, occupying 14.94% of the land, marking a significant increase compared to both 2015 and 2020. Additionally, barren land is categorized as covering 1.21% of the area, which reflects a noticeable decline from earlier years. Water bodies and developed areas constitute 3.68% and 1.44% of the land, respectively. While there have been slight decreases and increases in these categories, the changes are not substantial. This detailed analysis underscores the dynamic nature of the region's land use and cover over the studied period. The data also highlights the importance of continuous monitoring to understand and manage the environmental changes effectively.

Table 6. Results of LULC

Year	LULC Class	Area (ha)	Percentage (%)
2015	Water	22,390.84	4.41
	Developed	3,301.54	0.65
	Barren	36,405.31	7.16
	Forest	406,190.50	79.92
	Planted/Cultivated	39,977.30	7.87
2020	Water	19,764.94	3.89
	Developed	5,814.69	1.14
	Barren	23,582.83	4.64
	Forest	399,593.50	78.62
	Planted/Cultivated	59,509.19	11.71
2024	Water	18,687.30	3.68
	Developed	7,339.11	1.44
	Barren	6,150.84	1.21
	Forest	400,152.00	78.73
	Planted/Cultivated	75,938.20	14.94

The visualization of the Land Use Land Cover (LULC) for the year 2015, 2020 and 2024 were illustrated in the map below (see Figure 5), providing a clear representation of the study area's diverse landscape. This map categorizes the region into five major classes including water bodies, developed areas, barren land, forest, and planted/cultivated areas. Water bodies, depicted in blue, while developed areas, shown in red, indicate regions of urbanization or infrastructure. The barren land, marked in brown, identifies areas with little to no vegetation. The extensive forest cover, illustrated in dark green. Lastly, the planted/cultivated areas, shown in bright green, reflect agricultural activities within the region.

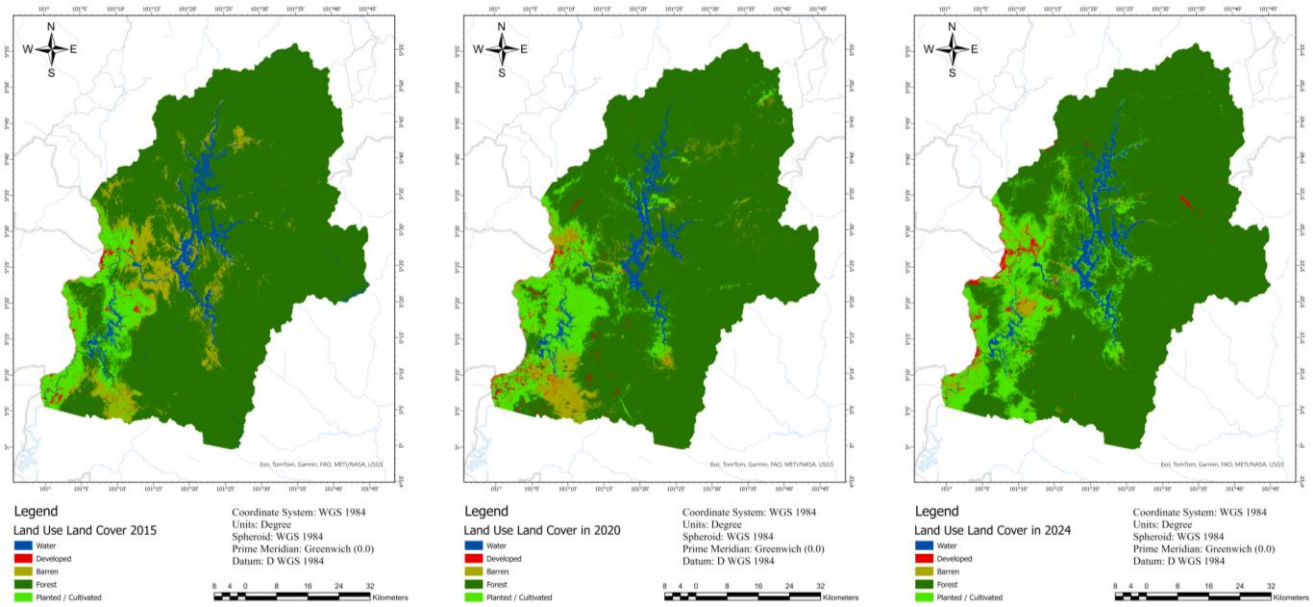

Figure 5. Results of LULC for 2015, 2020 and 2024

From the results of NDVI, LST, and LULC presented in Figure 3, Figure 4, and Figure 5, it can be concluded that these findings are consistent with patterns observed in similar tropical freshwater ecosystems. For example, land-use changes in the Dongting Lake area significantly influenced surface temperature distribution (Tan et al., 2020). Similarly, NDVI shifts caused by the spread of invasive aquatic vegetation were documented in Ethiopia's Lake Dambal (Godana et al., 2022), while land degradation in semi-arid regions of India showed strong correlations with both NDVI and LST variations (Kumar et al., 2022).

3.4. Water Quality

Water quality is one of the parameters that has been studied. Using Landsat 8 satellite imagery, water quality parameters were monitored by combining remote sensing with field observations. Reflectance values from Landsat 8/9 OLI/TIRS images were gathered and correlated with field data. Regression analysis identified the model to predict key water quality metrics. This integration of satellite and on-site data enabled the creation of models for estimating water quality. Relationship between spectral properties of Landsat 8 OLI/TIRS satellite bands and water quality parameters which include Ammoniacal Nitrogen (NH3), Biological Oxygen Demand (BOD), Total Suspended Solid (TSS), Dissolved Oxygen (DO), Temperature, Potential of Hydrogen (pH) and Turbidity has been obtained by applying regression analysis. The results of the regression analysis for the satellite band and the water quality parameters show a relationship between the spectral properties. The steps involved in doing this analysis were covered in the previous chapter. The resulting models for each parameter that were produced through multiple linear regression are displayed in Table 7 below.

The predictive models for water quality parameters were developed using multiple linear regression, incorporating in-situ observations from 2020 and corresponding Landsat satellite imagery data. Upon applying these models to the satellite data for the years 2015 and 2024, the predicted values were analyzed for accuracy

and relevance. The validation process involved comparing the predicted water quality parameters with available observed data to assess the model performance. Among the predicted parameters, three parameters of the water quality have demonstrated a strong relationship with the observed data, exhibiting high R-squared values. These parameters are Dissolve Oxygen (DO), pH and temperature.

Table 7. Derived Model for Each Parameter Through Regression Analysis

Water Quality	Derived Model	R^2
Ammoniacal Nitrogen	= 1.04 + 0.49 (B5) – 7.08 (B1)	0.46
Biological Oxygen Demand	= 22.18 – 4.25 (B5) – 178.83 (B1) + 57.76 (B4)	0.57
Total Suspended Solid	= -528.07 + 72.57 (B10) + 76.84 (B5) – 1056.13(B2)	0.61
Dissolve Oxygen	= 125.79 -15.11 (B10) + 115.70 (B1)	0.64
Temperature	= 56.23 -3.70 (B10) -807.30(B9) - 4.04 (B5) +84.66 (B1)	0.70
Potential of Hydrogen (pH)	= -14.40 +2.83 (B10) - 922.98 (B9) -3.59 (B5)	0.68
Turbidity	= -57.00 +10.73 (B11) +43.56 (B4) -213.87 (B1)	0.51

Figure 6 shows Water Quality Parameters (a) dissolved oxygen (b) pH and (c) Temperature in 2015. To conduct PCA in the subsequent step, only these three parameters that have been utilized to get the weightage to be assigned for weighted overlay analysis. Dissolved Oxygen (DO) levels ranged from 4.8 mg/L to 13.8 mg/L, while pH values varied between 8.1 and 10.6. Additionally, the water temperature during this period ranged from 32.7°C to 37.4°C.

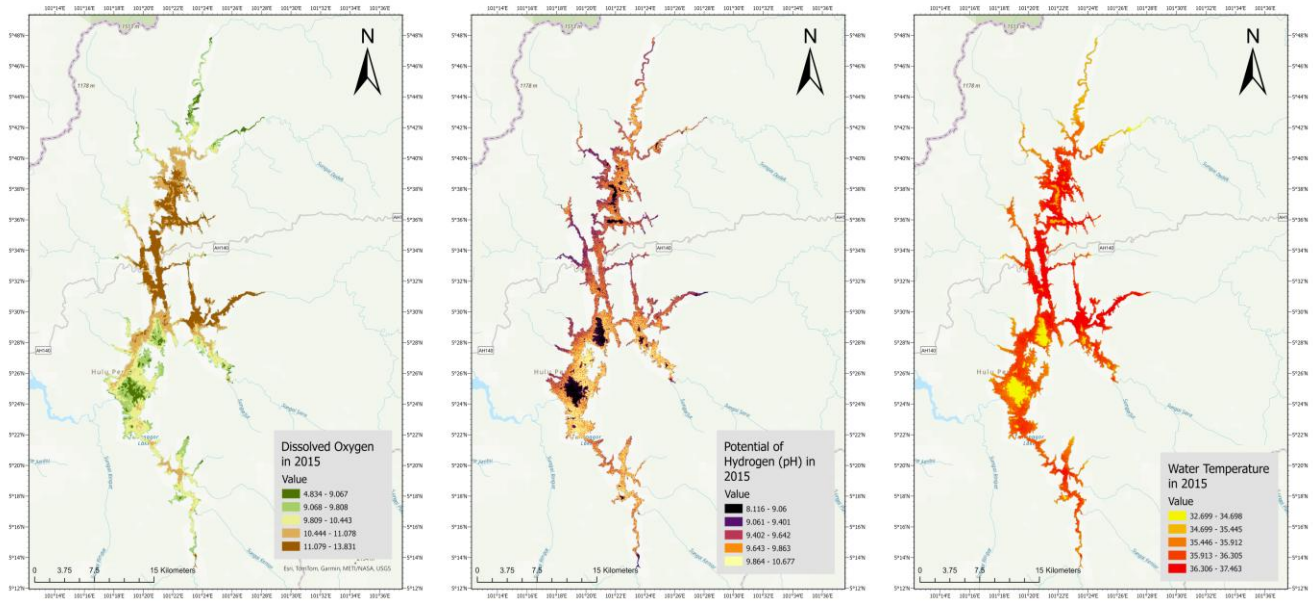

Figure 6. Water Quality Parameters (a) Dissolved Oxygen (b) pH and (c) Temperature in 2015

Figure 7 shows Water Quality Parameters (a) dissolved oxygen (b) pH and (c) Temperature in 2020. Among the anticipated parameters, these three water quality parameters showed a substantial relationship with the observed data, with high R-squared values. Hence, to conduct PCA in the subsequent step, only these three parameters that has been utilized to get the weightage to be assigned for weighted overlay analysis. Dissolved Oxygen (DO) levels ranged from 0.1 mg/L to 16.6 mg/L, while pH values varied between 3.6 and 9.7. Additionally, the water temperature during this period ranged from 24.4°C to 37.1°C.

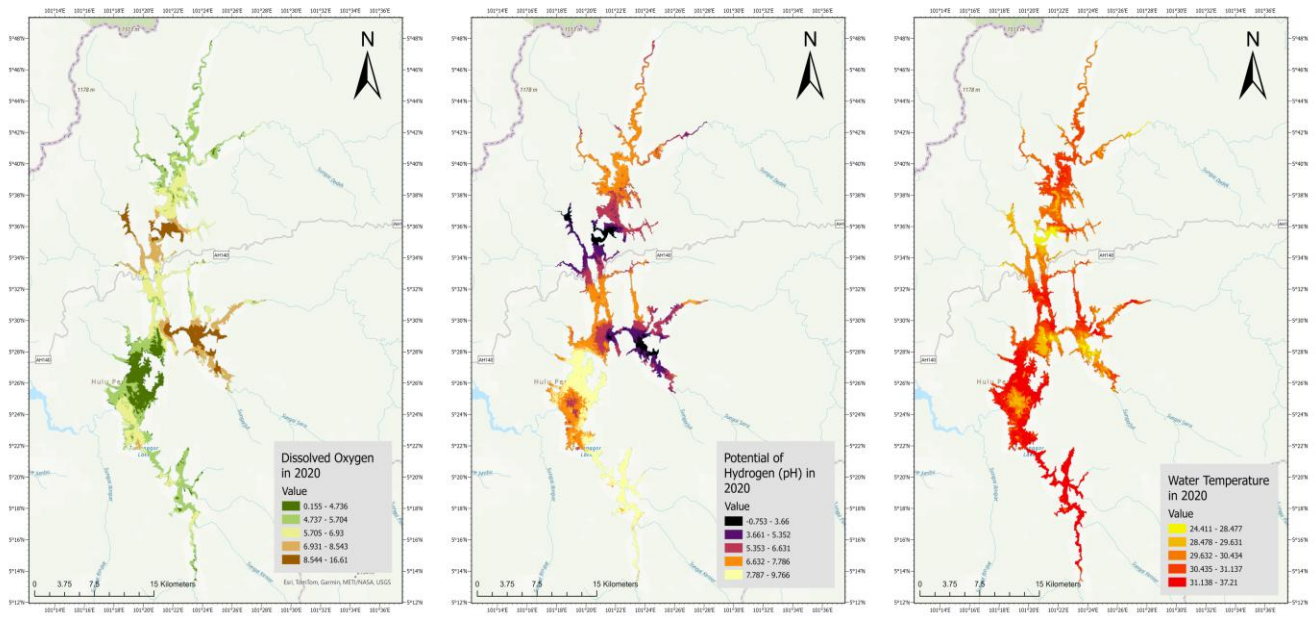

Figure 7. Water Quality Parameters (a) Dissolved Oxygen (b) pH and (c) Temperature in 2020

Figure 8 Water Quality Parameters (a) dissolved oxygen (b) pH and (c) Temperature in 2024. Among the anticipated parameters, these three water quality parameters showed a substantial relationship with the observed data, with high R-squared values. Hence, to conduct PCA in the subsequent step, only these three parameters that have been utilized to get the weightage to be assigned for weighted overlay analysis. Dissolved Oxygen (DO) levels ranged from 0.2 mg/L to 16.6 mg/L, while pH values varied between 3.6 and 9.7. Additionally, the highest water temperature during this period 29.3°C.

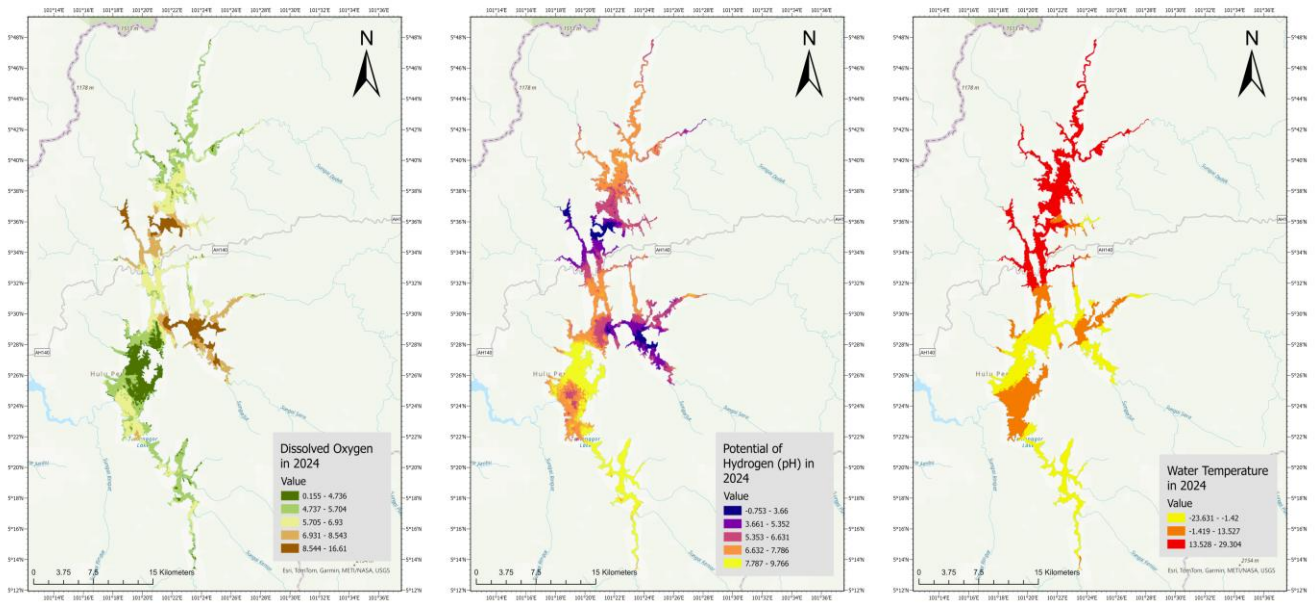

Figure 8. Water Quality Parameters (a) Dissolved Oxygen (b) pH and (c) Temperature in 2024

3.5. Air Temperature

Relationship between spectral properties of Landsat 8 OLI/TIRS satellite bands and air temperature has been obtained by applying regression analysis. The results of the regression analysis for the satellite band and air temperatures show a relationship between the spectral properties. The steps involved in doing this analysis have been covered in the previous chapter. The resulting models for air temperature that were produced through multiple linear regression are displayed in Table 8 below. Hence, the general form of equation to calculate air temperatures using Landsat 8 OLI/TIRS band were as follows:

Table 8. Derived Model for Air Temperature through Regression

Derived Model	R^2
AT = 45.57-1.36 (B11) -56.26 (B8)	0.32

The regression coefficients result between predicted and measured values of air temperature are ($AdjR^2$=0.32). This output indicates that approximately 32% of the variability in air temperature can be explained by the model. This suggests a moderate level of explanatory power, implying that while the model has some predictive capability, a significant portion of the variability in air temperature is influenced by factors not included in the model. Air temperature in 2015 has been predicted using the model derived from multiple linear regression earlier which the satellite band data involve is Band 8 and Band 11. The results of the multiple linear regression analysis are regarded acceptable because the model that was developed has shown effectiveness and reliability. This is demonstrated by its successful use in predicting air temperature for the following year. The consistency and accuracy of the predictions validate the model's effectiveness, indicating that it is suitable for ongoing and future analyses. Subsequently, to enhance the understanding and analysis of the air temperature results, the data has been classified using the Natural Breaks (Jenks) method. Given the variations in results, an approach was adopted to classify the data according to the appropriate readings for each year.

Table 9 show the classification ranges for the air temperature final output and Figure 9 depicts the visualization of air temperature data for the years 2015, 2020, and 2024 that have been predicted based on the model derived, respectively. The maps show a significant trend of very high temperatures across most of the region during these three years, with temperature ranges consistently exceeding 33 degrees Celsius. This persistent high-temperature pattern suggests a concerning level of thermal stress on the environment.

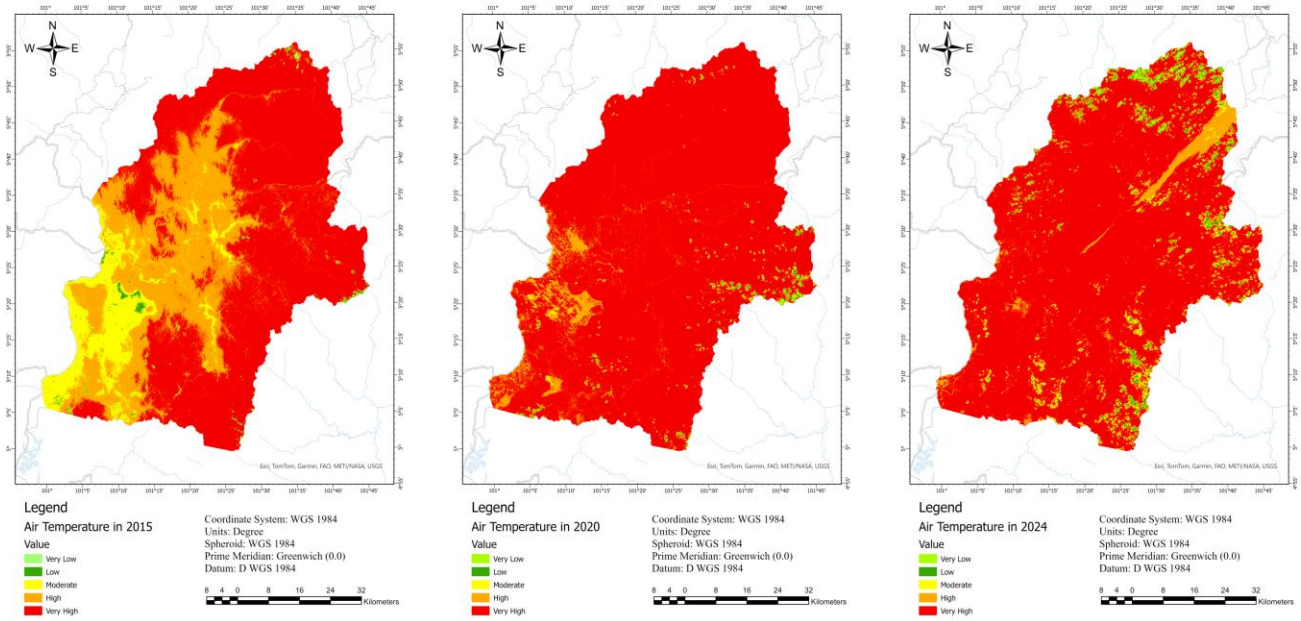

Figure 9. Results of Air Temperature in 2015, 2020 and 2024

Table 9. Classification Ranges for Air Temperatures

Class	Area (Ha)	LST Class
1	<10 °C	Very Low
2	10 – 19 °C	Low
3	19 – 26 °C	Moderate
4	26 – 29 °C	High
5	>33 °C	Very High

3.6. Determination of Environmental Degradation

Finally, after obtaining all the results of spatial data reproduction, the parameters will be utilized to assess environmental damage. Before progressing with subsequent processing, it is critical to classify all parameters in a more relevant and readable manner. The study then incorporates diverse environmental datasets, such as land use, water quality, and air temperatures, to produce a comprehensive collection. To add weights to the parameters of these variables, ArcGIS Pro's Principal Components tools have been used. Once the weights are set, the Weighted Overlay Analysis tool assigns a percentage weighting to each layer. A weighted overlay approach was used to further integrate the chosen parameters in order to operationalize the assessment of environmental degradation. This approach enables a thorough spatial assessment of environmental conditions by combining several environmental variables according to their relative importance. Figure 10 illustrates the reclassified criterion maps of each environmental parameter used as input layers for the weighted overlay analysis.

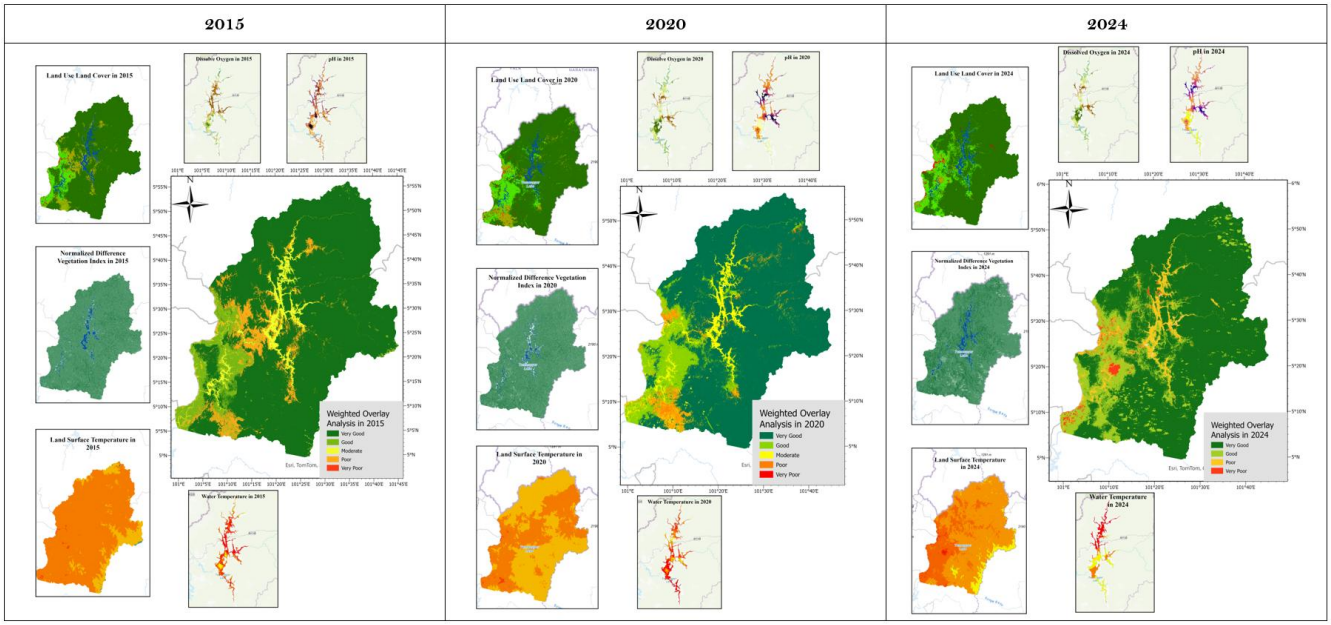

Figure 10. The Criterion Maps of the Environmental Condition Map of Tasik Temengor

The following table presents the key parameters utilized in this study to assess environmental degradation around Tasik Temenggor in Royal Belum, Perak. Each parameter has been assigned a weightage to facilitate the creation of maps through a weighted overlay analysis. The assignment of weightages reflects the relative importance of these parameters in influencing environmental conditions and degradation processes in the study area. The inclusion of relevant and significant criteria is important for the accuracy of weighted overlay analysis (WOA) in measuring environmental degradation. Air temperature was first considered as a criterion. However, subsequent analyses found that including it did not enhance the degradation prediction accuracy. This might be due to the insufficient number of ground sampling that has been collected in 2024. Since there are only 38 points, we need to predict them by using spatial interpolation only. Furthermore, Land Surface Temperature (LST) sufficiently captured the thermal properties impacting degradation, causing the inclusion of air

temperature redundant. This redundancy not only contributed little benefit, but also increased the chance of overlapping influences, which could distort the analysis. As a result, removing the air temperature from the WOA produced a more accurate and realistic degradation map. Thus, the PCA was conducted again, and the weightage used to generate the map is shown in Table 10.

Table 10. Weightage Assign for Parameters in 2015, 2020 and 2024

Year	Parameters	Weightage (%)
2015	Land Use Land Cover (LULC)	68
	Normalized Difference Vegetation Index (NDVI)	13
	Land Surface Temperatures (LST)	11
	Dissolve Oxygen (Water Quality)	7
	Ph (Water Quality)	1
2020	Land Use Land Cover (LULC)	57
	Normalized Difference Vegetation Index (NDVI)	15
	Land Surface Temperature (LST)	14
	Dissolve Oxygen (Water Quality)	11
	Ph (Water Quality)	3
2024	Land Use Land Cover (LULC)	58
	Normalized Difference Vegetation Index (NDVI)	16
	Land Surface Temperature (LST)	11
	Dissolve Oxygen (Water Quality)	9
	Ph (Water Quality)	4

The spatial distribution of environmental conditions in the study area was then examined using the weighted overlay results obtained from the chosen parameters (see Table 11),

Table 11. Spatial Distribution of Environmental Condition

Year	Class	Area (ha)	Percentage (%)
2015	Very Good	405297.3	79.77
	Good	40986.03	8.07
	Moderate	23895.76	4.7
	Poor	37906.91	7.46
	Very Poor	11.89399	0
2020	Very Good	397712.9	78.29
	Good	61961.02	12.2
	Moderate	31837.53	6.27
	Poor	16509.72	3.25
	Very Poor	0.215574	0
2024	Very Good	387141.3	76.25
	Good	88799.18	17.49
	Poor	24996.89	4.92
	Very Poor	6776.05	1.33

According to Table 11 and Figure 11, 79.77% of the region shows Very Good level of environmental condition. Referring to the LULC map from 2015, this area was predominantly forested, which explains its very good condition. This is understandable because forested areas are generally less impacted by human activities compared to urban or agricultural areas. Moreover, 8% of the total areas depict the area with good level of environmental conditions. This area has been identified as a planted/cultivated area from the land use classification results in 2015. Agricultural and managed lands often undergo regular maintenance and management practices that can mitigate environmental degradation factors such as erosion or habitat loss. Therefore, these areas would rationally show good environmental conditions. Furthermore, the water bodies area, including Tasik Temenggor, has been identified as having a moderate level of environmental condition, accounting for only 4% of the study area. Finally, 7% of the total area exhibits a poor level of environmental

condition, classified specifically as barren land. Barren land often refers to areas in which the vegetation or forest has been severely depleted or cannot be sustained due to a variety of environmental stresses such as soil degradation, desertification, or human activity such as deforestation. These variables contribute to poor levels of environmental condition than places with natural vegetation or managed landscapes.

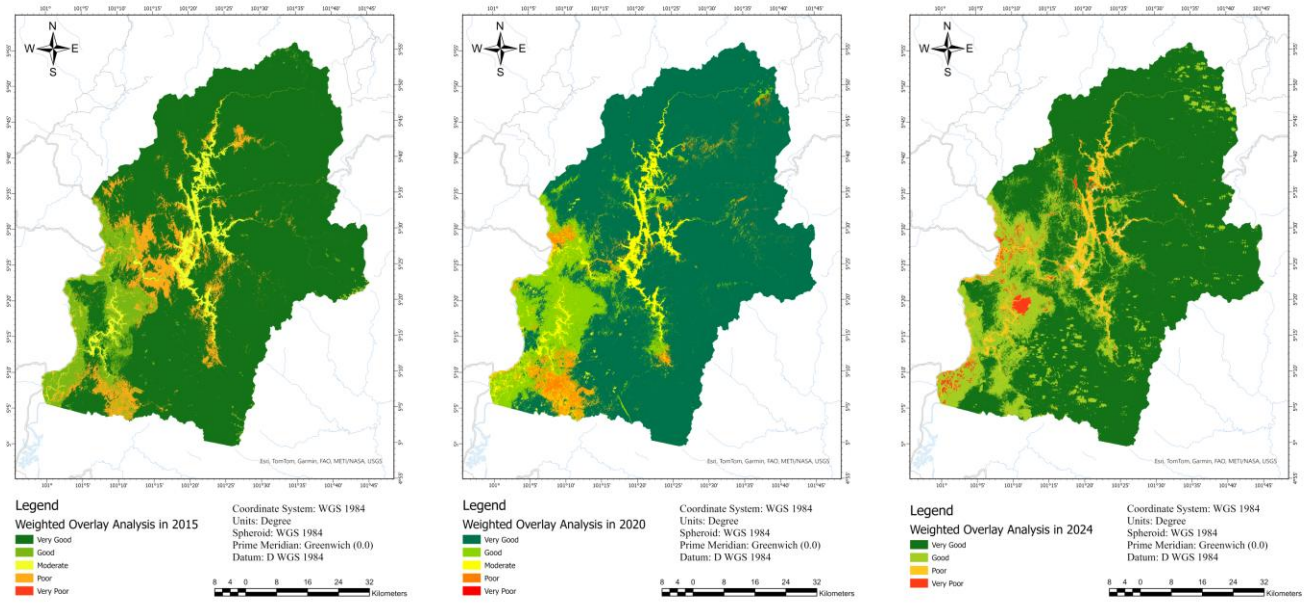

Figure 11. The Environmental Condition of Tasik Temenggor, Perak in 2015, 2020 and 2024

Based on the data in Table 11, 78.29% of the region exhibits a Very Good environmental condition. According to the 2020 LULC map, this area was mostly covered by forests, which accounts for its minimal environmental impact. However, the slight decrease in percentage compared to the previous year suggests that some degradation has occurred in the area. Furthermore, 12% of the total area is classified as having a good environmental condition, identified as planted or cultivated areas according to the 2020 land use classification. Compared to the previous year's analysis, the increase from 8% in 2015 to 12% in 2020 suggests an improvement. This shift likely indicates that areas previously categorized as 'moderate' have improved to the 'good' category. Furthermore, 6.3% of the total area, classified as having a moderate environmental condition, includes water bodies and developed areas based on the 2020 LULC map. Compared to the previous year's analysis, it can be inferred that this area has experienced degradation, as indicated by the increase in moderate condition areas from 4.7% in 2015 to 6.3% in 2020. Finally, 3.2% of the total area exhibits a Poor level of environmental condition, classified specifically as barren land and developed area. They are classified as poor environmental conditions due to their significant transformation from natural ecosystems, associated environmental impacts, and human activities. However, this area could be considered improved this year, as the percentage of poor level of environmental conditions has decreased from 7% to 3.2%.

Based on the data in Table 11, 76.25% of the region reveals a Very Good condition of the area. According to the 2024 LULC map, this area was mostly covered by forests. However, the slight decrease in percentage compared to the previous year suggests that some degradation has occurred in the area. Furthermore, 17.49% of the total area represents areas with Good environmental condition, identified as planted or cultivated areas based on the 2024 land use classification results. The percentage of areas classified as having a good environmental condition increased from 12% in 2020 to 17.49% in 2024. Hence, this improvement suggests that more areas have transitioned to a higher quality environmental condition over the years. In addition, 4.92% of the study area exhibits a Poor environmental condition. This category includes water bodies, including Tasik Temenggor, as well as areas classified as developed based on the LULC map in 2024. By comparing the classification from the previous year, we can conclude that water bodies area has been experiencing degradation, same indicator

also being used by other studies (Qin et al., 2024; Shi et al., 2024). Finally, 1.33% of the total area exhibits a Very Poor condition, specifically classified as barren land and developed area. Barren land and developed areas are classified as displaying Very Poor environmental condition due to their significant transformation from natural ecosystems, associated environmental impacts, and human activities (Shooshtari & Jahanishakib, 2024; Wei et al., 2020). By comparing the percentage of having a very poor condition with the previous year, this year seems to experience degradation since the area percentage has been increasing.

Additionally, Figure 12 illustrates the visible insitu stress signs for four selected sites that shows the most significant environmental degradation of the study area since 2015 until 2024. This figure zooms into several key sites, showcasing the evolution of surface conditions within the study area. Visible signs of environmental stress, such as land clearing, deforestation, and land conversion, reveal consistent degradation across the region over the past decade. When zooming into specific sites, Site A displays extensive deforestation, which aligns with the LULC results indicating that the area has shifted from planted/cultivated land to barren land. This transformation suggests a significant decline in land productivity, likely due to unsustainable land use practices, soil degradation, or abandonment following intensive agricultural activities (Zhou et al., 2022). These situations resulted in a large decrease in NDVI over time. Therefore, if forests are destroyed and the land becomes barren, the NDVI will decrease, suggesting a loss of biomass and vegetation cover. As vegetation declines, LST is anticipated to rise. Vegetation regulates temperature by providing shade and transpiring water, which cools the surface. The transition to bare land, with its exposed soil, would raise surface temperatures due to increased sun absorption and decreased evapotranspiration.

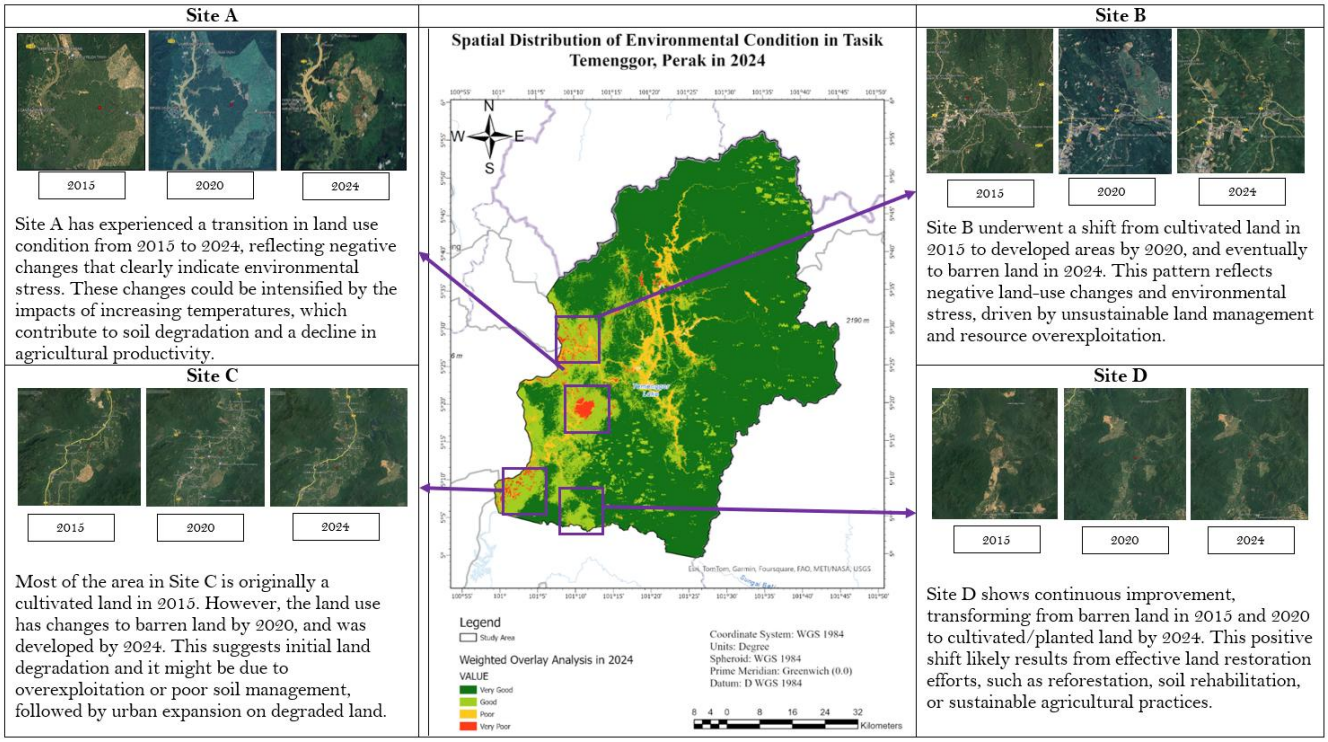

Figure 12. The In-Situ Visible Sign of Stress of Tasik Temenggor, Perak in 2015, 2020 and 2024

Additionally, Site B experienced a shift from cultivated land in 2015 to more developed areas by 2020, followed by an increase in barren land in 2024, located in the same areas as the developed land. This pattern indicates negative land-use changes and is a clear sign of environmental stress. The progression from cultivation to development, and ultimately to land degradation, suggests unsustainable land management practices and possible overexploitation of resources. The transition from cultivated land to developed areas in 2020 would result in a moderate reduction in NDVI since developed areas typically have less vegetation. The further

transition to barren land by 2024 will result in an even sharper reduction in NDVI, reflecting the deterioration and lack of vegetation (Karim et al., 2023). Initially, the expansion of built-up regions would result in an increase in LST because urban surfaces absorb more heat than vegetated land. By 2024, when the land becomes barren, LST may remain high or perhaps rise further due to the lack of vegetation to cool the surface via evapotranspiration (Qiu et al., 2013; Yu et al., 2024)

Furthermore, Site C experienced a shift from cultivated land in 2015 to barren land by 2020, and by 2024, the area had been developed. This progression suggests that the initial land degradation may have been caused by overexploitation or poor soil management, leading to abandonment. The subsequent development likely took advantage of the degraded land for urban or infrastructure expansion, indicating a lack of sustainable land-use practices and possibly driven by economic or demographic factors. The conversion from cultivated to barren land by 2020 would result in a considerable decline in NDVI due to crop and plant loss. By 2024, growth in the area may further diminish NDVI values, while certain types of development may balance this slightly. Overall, NDVI suggests a long-term deterioration in vegetation health. As the terrain changes from cultivated to barren land, the LST rises due to a lack of vegetation. As the area develops, the LST may continue to rise as urban surfaces contribute to the urban heat island effect, raising temperatures even higher (Tan et al., 2020).

Finally, Site D exhibits continuous improvement. In 2015, the area was predominantly barren, and by 2020, the extent of barren land had increased. By 2024, however, the area had transformed into cultivated/planted land. This improvement is likely the result of successful land restoration efforts, such as reforestation, soil rehabilitation, or sustainable agricultural practices, indicating a positive shift towards more productive land use and effective environmental management strategies. Site D demonstrates ongoing improvement, with the region transitioning from barren land between 2015 and 2020 to cultivated land in 2024. NDVI values would initially be low due to the empty area, but they would grow dramatically by 2024 as the land was cultivated and vegetation increased. The increase in NDVI indicates a healthy trend in vegetation. The lack of vegetative cover in this dry climate would have initially resulted in a high LST (Isa et al., 2018). However, as the ground is recovered and planted with crops or other vegetation, LST will decrease due to the cooling effects of plant evapotranspiration and increased shading. A drop in LST would also suggest an improvement in environmental conditions and hence influence of the human anthropogenic activities (Liu et al., 2020).

To conclude, the reasons for environmental degradation and improvement at Sites A, B, C, and D are directly linked to changes in NDVI and LST. Decreased NDVI and increased LST typically imply environmental stress, such as deforestation and land degradation, as observed in Sites A, B, and C. In contrast, increases in NDVI and decreases in LST, as seen at Site D, indicate good environmental changes such as reforestation, land restoration, or sustainable agriculture methods. These indicators give a quantitative framework for assessing the land's health and surface conditions throughout time.

The findings of this study contribute significantly to the growing body of research on environmental degradation assessment using geospatial technology. By integrating Principal Component Analysis (PCA) and Weighted Overlay Analysis (WOA) within a GIS framework, this research presents a comprehensive, multi-parameter approach that enables spatially and temporally explicit mapping of environmental degradation. Compared to previous studies that analyzed only one or two parameters in isolation such as land use or NDVI this study simultaneously examines NDVI, LST, LULC, and water quality, providing a more holistic understanding of ecological change. The spatio-temporal degradation trends observed in Tasik Temenggor, particularly the correlation between forest conversion and increased surface temperature and vegetation decline, are consistent with studies conducted in China (Zhou et al., 2022), Vietnam (Karim et al., 2023), and Ethiopia (Godana et al., 2022). However, the integration of remote sensing with in-situ validation and PCA-weighted modeling distinguishes this work from previous efforts. The methodological framework demonstrated here not only enhances local-level environmental assessments but also contributes theoretically by showcasing how geospatial multi-variable synthesis can be operationalized to detect, explain, and visualize degradation patterns across time. This level of integration represents a novel and scalable approach for future applications in other freshwater ecosystems and protected areas.

4. Conclusion

In summary, this study has provided a comprehensive study of environmental degradation in the Tasik Temenggor region, employing a combination of geospatial techniques and statistical analyses to uncover significant insights. Through the systematic identification of key variables such as NDVI, LST, LULC, water quality, and air temperature, and the application of spatio-temporal analyses, the study has developed a detailed understanding of the factors driving environmental change in this ecosystem. The integration of remote sensing data with in-situ measurements has proven particularly effective in creating a methodology for assessing environmental conditions, concluding in a comprehensive map that visualizes the spatial distribution of degradation, which similar condition also exhibited at other regions.

The approach has highlighted the effectiveness of geospatial technology in environmental monitoring, yet several areas for improvement and future research have been identified. Incorporating machine learning techniques alongside traditional statistical methods can enhance the ability to handle large datasets and uncover complex patterns. Algorithms like Random Forest, Support Vector Machines (SVM), and Neural Networks can provide deeper insights and improve predictive accuracy. Additionally, employing advanced geospatial tools such as Google Earth Engine for large-scale data processing and ArcGIS Pro for detailed spatial analysis can refine monitoring capabilities by managing multi-dimensional data from various sensors more precisely and efficiently. Future studies should also expand the temporal scope to include longer time periods, offering a more comprehensive view of environmental trends and changes, while more frequent data collection intervals would enhance the granularity and reliability of the findings.

Integrating high-resolution remote sensing platforms like Sentinel, MODIS, and Landsat allows for continuous monitoring and detection of subtle environmental changes. When combined with geospatial techniques like kriging and hotspot analysis, these tools can significantly enhance the accuracy of mapping pollutant concentrations and other critical environmental indicators. Future research should focus on translating these findings into actionable environmental policies and targeted conservation strategies, especially in the most ecologically vulnerable areas. Despite these methodological strengths, the study does face several limitations. The spatial resolution of Landsat imagery (30m) may be insufficient to capture fine-scale variations, and the limited number of in-situ water quality sampling points (only six stations) may underrepresent spatial variability across the lake. Additionally, masking due to cloud cover in the 2024 imagery may have introduced spatial data gaps. Future studies are encouraged to incorporate higher-resolution sensors like Sentinel-2 and to increase both the frequency and spatial density of field observation. Overall, this research offers a strong foundation for assessing environmental degradation in Tasik Temenggor. However, further refinement particularly through the adoption of advanced analytical techniques and closer integration with conservation practice will be essential to support the long-term sustainability of this critical ecosystem.

5. Acknowledgments

The author would like to acknowledge and express their incredible gratitude to the Universiti Teknologi MARA for the financial support provided under the Matching Grant Scheme 600-TNCPI 5/3/DDN (10) (003/2023). Operational Land Imager (OLI) Level-1T data were obtained from U.S. Geological Survey (USGS), which has made all Landsat data freely available for this work and future research.

6. References

Albert, J. S., Destouni, G., Duke-Sylvester, S. M., Magurran, A. E., Oberdorff, T., Reis, R. E., Winemiller, K. O., & Ripple, W. J. (2021). Scientists' Warning to Humanity on the Freshwater Biodiversity Crisis. *Ambio*, *50*(1), 85–94. [Crossref]

Arshad, N., Rahman, A. T. A., Jafar, S. M., Aziz, N. W., & Osman, R. (2022). Assessment of Water Quality in the Temenggor Forest Reserve based on Physicochemical Data and Elemental Content. *Malaysian Journal of Chemistry*, *24*(2), 1–11. [Crossref]

Godana, G., Fufa, F., & Debesa, G. (2022). Eichhornia Crassipes Expansion Detection Using Geospatial Techniques: Lake Dambal, Oromia, Ethiopia. *Environmental Challenges*, *9*, 100616. [Crossref]

Ho, L. T., & Goethals, P. L. M. (2019). Opportunities and Challenges for the Sustainability of Lakes and Reservoirs in Relation to the Sustainable Development Goals (SDGs). *Water*, *11*(7), 1462. [Crossref]

Isa, N. A., Wan Mohd, W. M. N., Salleh, S. A., & Ooi, M. C. G. (2018). The Effects of Green Areas on Air Surface Temperature of the Kuala Lumpur City Using WRF-ARW Modelling and Remote Sensing Technique. *IOP Conference Series: Earth and Environmental Science*, *117*, 012012. [Crossref]

Kamaruzzaman, K., Salleh, S. A., Pardi, F., Abdullah, M. F., Foronda, V., Bergonio, E. L., & Rahmawaty, R. (2025). Review of Environmental Monitoring in Freshwater Lakes Using Geospatial Techniques (Remote Sensing and GIS). *Geocarto International*, *40*(1). [Crossref]

Karim, M., Deng, J., Ayoub, M., Dong, W., Zhang, B., Yousaf, M. S., Bhutto, Y. A., & Ishfaque, M. (2023). Improved Cropland Abandonment Detection with Deep Learning Vision Transformer (DL-ViT) and Multiple Vegetation Indices. *Land*, *12*(10), 1926. [Crossref]

Kowe, P., Ncube, E., Magidi, J., Ndambuki, J. M., Rwasoka, D. T., Gumindoga, W., Maviza, A., de jesus Paulo Mavaringana, M., & Kakanda, E. T. (2023). Spatial-Temporal Variability Analysis of Water Quality Using Remote Sensing Data: A Case Study of Lake Manyame. *Scientific African*, *21*, e01877. [Crossref]

Kumar, B. P., Babu, K. R., Anusha, B. N., & Rajasekhar, M. (2022). Geo-Environmental Monitoring and Assessment of Land and Desertification in the Semi-Arid Regions Using Landsat 8 OLI / TIRS, LST, and NDVI Approach. *Environmental Challenges*, *8*, 100578. [Crossref]

Liu, S., Li, X., Chen, D., Duan, Y., Ji, H., Zhang, L., Chai, Q., & Hu, X. (2020). Understanding Land use/Land Cover Dynamics and Impacts of Human Activities in the Mekong Delta Over the last 40 years. *Global Ecology and Conservation*, *22*, e00991. [Crossref]

Martinsen, K. T., & Sand-Jensen, K. (2022). Predicting Water Quality from Geospatial Lake, Catchment, and Buffer Zone Characteristics in Temperate Lowland Lakes. *Science of The Total Environment*, *851*, 158090. [Crossref]

Muchini, R., Gumindoga, W., Togarepi, S., Masarira, T. P., & Dube, T. (2018). Near Real Time Water Quality Monitoring of Chivero and Manyame Lakes of Zimbabwe. *Proceedings of the International Association of Hydrological Sciences*, *378*, 85–92. [Crossref]

Nagy A, Szabó A, Adeniyi OD, Tamás J (2021) Wheat Yield Forecasting for the Tisza River Catchment Using Landsat 8 NDVI and SAVI Time Series and Reported Crop Statistics. Agronomy 11:652. [Crossref]

Nisar, A., Mahmood, S., & Shakoor, M. (2023). Spatio-Temporal Analysis of Snow Cover Change in Hunza Valley, Karakoram Region. *Advanced Remote Sensing*, *3*(2), 58–68.

Pratama, M. R. A., Manessa, M. D. M., Supriatna, S., Ayu, F., & Haidar, M. (2022). Spatial Distribution of Coral Reef Degradation with Human Activities in the Coastal Waters of Samatellu Lompo Island, South Sulawesi. *Geoplanning: Journal of Geomatics and Planning*, *9*(2), 121–132. [Crossref]

Qin, X., Yang, Q., & Wang, L. (2024). The Evolution of Habitat Quality and its Response to Land Use Change in the Coastal China, 1985–2020. *Science of The Total Environment*, *952*, 175930. [Crossref]

Qiu, G., Li, H., Zhang, Q., Chen, W., Liang, X., & Li, X. (2013). Effects of Evapotranspiration on Mitigation of Urban Temperature by Vegetation and Urban Agriculture. *Journal of Integrative Agriculture*, *12*(8), 1307–1315. [Crossref]

Razak, M. F. A., Osnin, N. A., Rahman, N. S. F. A., Hamid, S. A., & Saman, A. K. A. (2020). Safety Assessment of Passenger Boat and Houseboat at Temenggor Lake, Malaysia. *International Journal of Scientific & Technology Research*, *9*(5), 262–266.

Rodell, M., Famiglietti, J. S., Wiese, D. N., Reager, J. T., Beaudoing, H. K., Landerer, F. W., & Lo, M.-H. (2018). Emerging Trends in Global Freshwater Availability. *Nature*, *557*(7707), 651–659. [Crossref]

Salleh, S.A., Latif, Z. A., Pradhan, B., Wan Mohd, W. M. N., & Chan, A. (2014). Functional Relation of Land Surface Albedo with Climatological Variables: a Review on Remote Sensing Techniques and Recent Research developments. *Geocarto International*, *29*(2), 147–163. [Crossref]

Salleh, Siti Aekbal, Latif, Z. A., Chan, A., Morris, K. I., Ooi, M. C. G., & Mohd, W. M. N. W. (2015). Weather Research Forecast (WRF) Modification of Land Surface Albedo Simulations for Urban Near Surface Temperature. *2015 International Conference on Space Science and Communication (IconSpace)*, 243–247. [Crossref]

Shi, X., Mao, D., Song, K., Xiang, H., Li, S., & Wang, Z. (2024). Effects of Landscape Changes on Water Quality: A Global Meta-Analysis. *Water Research*, *260*, 121946. [Crossref]

Shooshtari, S. J., & Jahanishakib, F. (2024). Estimating the Severity of Landscape Din future Management Scenarios based on Modeling the Dynamics of Hoor Al-Azim International Wetland in Iran-Iraq Border. *Scientific Reports*, *14*(1), 11877. [Crossref]

Tan, J., Yu, D., Li, Q., Tan, X., & Zhou, W. (2020). Spatial Relationship between Land-Use/Land-Cover Change and Land Surface Temperature in the Dongting Lake Area, China. *Scientific Reports*, *10*(1), 9245. [Crossref]

Tibebe, D., Zewge, F., Lemma, B., & Kassa, Y. (2022). Assessment of Spatio-Temporal Variations of Selected Water Quality Parameters of Lake Ziway, Ethiopia Using Multivariate Techniques. *BMC Chemistry*, *16*(1), 11. [Crossref]

Topp, S. N., Pavelsky, T. M., Jensen, D., Simard, M., & Ross, M. R. V. (2020). Research Trends in the Use of Remote Sensing for Inland Water Quality Science: Moving Towards Multidisciplinary Applications. *Water*, *12*(1), 169. [Crossref]

Tran, H., Tran, T., & Kervyn, M. (2015). Dynamics of Land Cover/Land Use Changes in the Mekong Delta, 1973–2011: A Remote Sensing Analysis of the Tran Van Thoi District, Ca Mau Province, Vietnam. *Remote Sensing*, *7*(3), 2899–2925. [Crossref]

Wei, W., Gao, Y., Huang, J., & Gao, J. (2020). Exploring the Effect of Basin Land Degradation on Lake and Reservoir Water Quality in China. *Journal of Cleaner Production*, *268*, 122249. [Crossref]

Xie, G., & Niculescu, S. (2021). Mapping and Monitoring of Land Cover/Land Use (LCLU) Changes in the Crozon Peninsula (Brittany, France) from 2007 to 2018 by Machine Learning Algorithms (Support Vector Machine, Random Forest, and Convolutional Neural Network) and by Post-classification C. *Remote Sensing*, *13*(19), 3899. [Crossref]

Yu, Z., Chen, J., Chen, J., Zhan, W., Wang, C., Ma, W., Yao, X., Zhou, S., Zhu, K., & Sun, R. (2024). Enhanced Observations from an Optimized Soil-Canopy-Photosynthesis and Eflux Model Revealed Evapotranspiration-Shading Cooling Dynamics of Urban Vegetation During Extreme Heat. *Remote Sensing of Environment*, *305*, 114098. [Crossref]

Zhou, J., Leavitt, P. R., Zhang, Y., & Qin, B. (2022). Anthropogenic Eutrophication of Shallow L: Is it Occasional? *Water Research*, *221*, 118728. [Crossref]